Natural Resources Canada
Ressources naturelles Canada

GEOLOGICAL SURVEY OF CANADA
OPEN FILE 8798

Uranium enrichment processes in metasomatic iron oxide and alkali-calcic systems as revealed by uraninite trace element chemistry—supplementary data

E.G. Potter, P. Acosta-Góngora, L. Corriveau, J-F. Montreuil, and Z. Yang

2021

Canada

GEOLOGICAL SURVEY OF CANADA
OPEN FILE 8798

Uranium enrichment processes in metasomatic iron oxide and alkali-calcic systems as revealed by uraninite trace element chemistry—supplementary data

E.G. Potter[1], P. Acosta-Góngora[1], L. Corriveau[2], J.-F. Montreuil[3], and Z. Yang[1]

[1]Geological Survey of Canada, 601 Booth Street, Ottawa, Ontario
[2]Geological Survey of Canada, 490 rue de la couronne, Québec, Quebec
[3]formerly Institut National de la Recherche Scientifique (INRS), 490 rue de la couronne, Québec, Quebec, current address: Red Pine Exploration Inc., 145 Wellington Street West, Suite 1001, Toronto, Ontario.

2021

Permanent link: https://doi.org/10.4095/328300

This publication is available for free download through GEOSCAN (https://geoscan.nrcan.gc.ca/).

Recommended citation
Potter, E.G., Acosta-Góngora, P., Corriveau, L., Montreuil, J.-F., and Yang, Z., 2021. Uranium enrichment processes in metasomatic iron oxide and alkali-calcic systems as revealed by uraninite trace element chemistry—supplementary data; Geological Survey of Canada, Open File 8798, 1 .zip file. https://doi.org/10.4095/328300

Publications in this series have not been edited; they are released as submitted by the author

Introduction

This report provides supplementary data (electron probe microanalysis and laser ablation-inductively coupled plasma-mass spectrometry) of uraninite grains for Potter et al. (*in press*). In Potter et al. (*in press*), uraninite from IOCG and affiliated mineral occurrences from the Great Bear magmatic zone in Canada (Fig. 1) was examined to gain insights on the metal sourcing and precipitation mechanisms in the deposits. This setting is an ideal natural laboratory to study uranium enrichment in these metasomatic systems, as excellent glaciated exposures of the weakly to non-deformed and unmetamorphosed occurrences illustrate the evolution from IOA (Hildebrand, 1986) to magnetite, magnetite-hematite and hematite group IOCG deposits (Corriveau et al., 2010, 2016; Mumin et al., 2010; Ootes et al., 2010; Potter et al., 2013; Richards and Mumin, 2013; Montreuil et al., 2016a, b). The regional-scale systems also host a wide spectrum of affiliated deposits such as albitite-hosted uranium (Montreuil et al., 2015, 2016b; Potter et al., 2019), skarn (Gandhi, 2003; Williams, 2010; Corriveau et al., *in press*) and epithermal-style veins (Mumin et al., 2010; Somarin and Mumin, 2012; Gandhi et al., 2018). As documented by several authors (e.g. Fryer and Taylor, 1987; Pagel et al., 1987; Maas and McCulloch, 1990; Hidaka et al., 1992; Fayek and Kyser, 1997; Hidaka and Gauthier-Lafaye, 2001; Cuney, 2010; Mercadier et al., 2011; Frimmel et al., 2014; Spano et al., 2017; Duffet et al., 2020), the trace element chemistry of uraninite is unique to the deposit type and provenance associated with its formation, and reflects the conditions under which the mineral crystallized (combination of fluid chemistry, temperature, source materials, etc.). As such, the chemistry of uraninite, coupled with field relationships and petrography, can provide insights on the sourcing and precipitation of uranium in these systems.

Methods

Thick (~200 μm) polished thin sections were prepared from polished sample slabs, using autoradiographs to target uraninite grains. The target grains were examined using a Zeiss EVO 50 series Scanning Electron Microscope (SEM) equipped with a Backscattered Electron Detector at the Geological Survey of Canada (GSC) in Ottawa. The Oxford energy dispersive spectrometry (EDS) system includes the X-MAX 150 Silicon Drift Detector, the INCA Energy 450 software and the latest AZtec microanalysis software. The SEM was operating at 20 kV with a beam current of 400 pA to 1 nA. Uraninite grains were analyzed with a Cameca SX50 electron microprobe at the GSC and a JEOL 8230 electron microprobe at the University of Ottawa. Operating conditions were 20 kV accelerating voltage and 10 nA current, with 20 s on peak and 10 s off-peak counting times. A mixture of natural and synthetic pure metal, simple oxides and simple compounds were used as standards. Data reduction was accomplished with a ZAF matrix correction

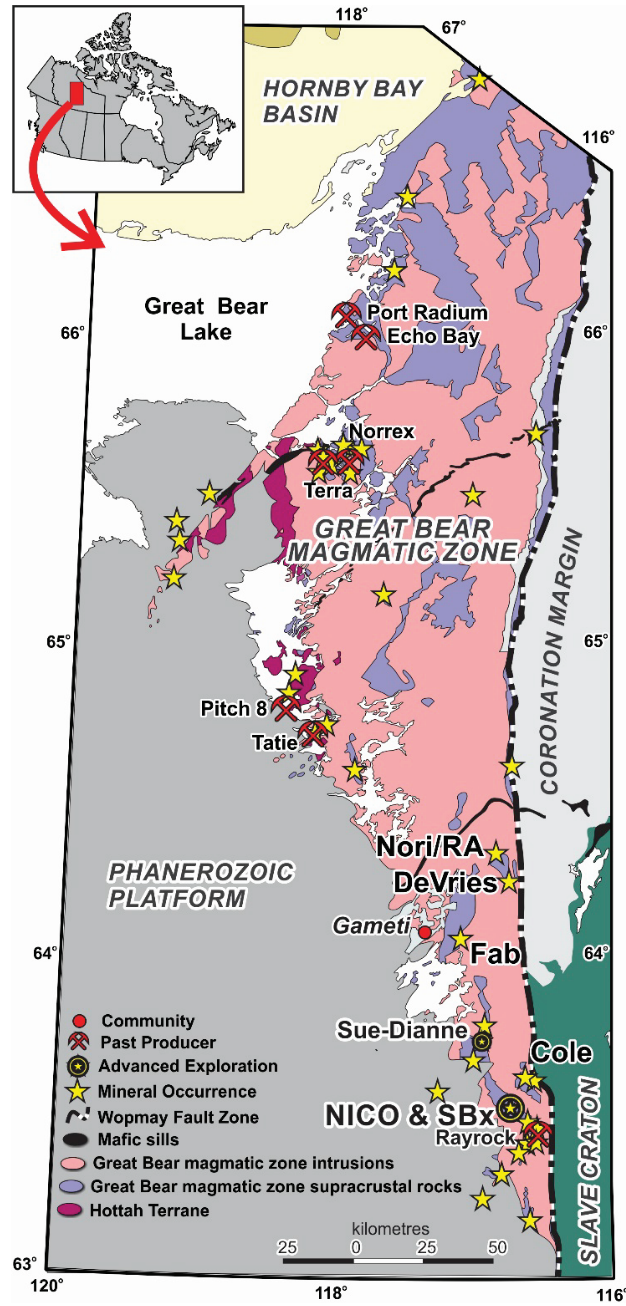

FIGURE 1. Location of the Great Bear magmatic zone and mineral occurrences examined in this study (bold font). Geology after Hoffman and Hall (1993) and mineral occurrences from the NORMIN database (www.nwtgeoscience.ca/normin).

using Probe For Windows software (Armstrong, 1988) and Pouchou and Pichoir (1984) using JEOL software. For elements with concentrations <1 wt.%, typical detection limits during electron microprobe analysis were: 0.17 wt% ThO_2, 0.08 wt% Y_2O_3, 0.25 wt% La_2O_3, 0.03 wt% CaO, and 0.04 wt% FeO.

Trace element concentrations were analyzed using *in situ* laser ablation-inductively coupled plasma-mass spectrometry (LA-ICP-MS) on polished thick sections at the

GSC. The system consists of a Teledyne-Photon Machines Analyte G1 excimer laser (193 nm) ablation system with a Helex dual-volume ablation cell and an Agilent 7700x quadrupole ICP-MS equipped with a second rotary vacuum pump that improves instrument sensitivity across the mass range by ~2 times (Jackson and Cabri, 2011). Analyses were done using a 26 µm spot size at repetition rate of 10 Hz, and a fluence of 4.53 J/cm^2 for the 200 µm thick polished sections. Helium gas was used to transport ablated sample material from the ablation cell. The sample and He mixture was mixed with argon (flow rate of 1.05 L/min) before entering the ICP-MS. Data acquisition time was 100 s in length, including 40 s of background signal prior to ablation and 60 s of sample signal. A USGS doped basaltic glass GSE-1G standard (Guillong et al., 2005) was used as calibration standard, while BCR-2G was used as a quality control standard, following methods outlined in Jackson (2008). The data reduction was performed using GLITTER (Griffin et al., 2008). The "GeoReM preferred values" (as of February 2010) from the on-line geological and environmental reference materials database (GeoReM; Jochum et al., 2005) were used for the concentrations of the elements in GSE-1G and BCR-2G. Most elements were within 5–10% of the accepted values for GSE-1G, except for Tb, Tm and Lu which within 15%. Average lower detection limits for REE during uraninite analyses were (in ppm): La=0.004, Ce=0.009, Pr=0.004, Nd=0.025, Sm=0.022, Eu=0.006, Gd=0.032, Tb=0.002, Dy=0.011, Ho=0.004, Er=0.021, Tm=0.002, Yb=0.012, Lu=0.003. The uranium content determined by electron probe microanalysis (EPMA) was used as an internal standard. The integrated region of sample signal was selected carefully to exclude regions associated with inclusions and/or ablation of surrounding minerals. In addition to the aforementioned standards, trace element concentrations were verified against a well-characterized uraninite from Mistamisk, Quebec (Bonhoure et al., 2007; Mercadier et al., 2011; Lach et al., 2013).

References

Armstrong, J.T., 1988. Quantitative analysis of silicates and oxide minerals: comparison of Monte-Carlo, ZAF and Phi-Rho-Z procedures; *in* Microbeam analysis, (ed.) D.E. Newbury; San Francisco Press, p. 239–246.

Bonhoure, J., Kister, P., Cuney, M., and Deloule, E., 2007. Methodology for rare earth element determinations of uranium oxides by ion microprobe; Geostandards and Geoanalytical Research, v. 31, p. 209–225.

Corriveau, L., Williams, P.J., and Mumin, A.H., 2010. Alteration vectors to IOCG mineralisation – from uncharted terranes to deposits; *in* Exploring for iron oxide copper-gold deposits: Canada and global analogues, (ed.) L. Corriveau A.H. Mumin; Geological Association of Canada, Short Course Notes, No. 20, p. 89–110.

Corriveau, L., Montreuil, J.-F., and Potter, E.G., 2016. Alteration facies linkages among IOCG, IOA and affiliated deposits in the Great Bear magmatic zone, Canada; *in* Proterozoic iron oxide-apatite (± REE) and iron oxide-copper-gold and affiliated deposits of Southeast Missouri, USA, and the Great Bear magmatic zone, Northwest Territories, Canada, (ed.) J. Slack, L. Corriveau and M. Hitzman; Economic Geology, v. 111, p. 2045–2072.

Corriveau, L., Mumin, A.H., and Potter, E.G., in press. Mineral systems with iron oxide-copper-gold (Ag-Bi-Co-U-REE) and affiliated deposits: introduction and overview; *in* Mineral systems with iron oxide-copper-gold (IOCG) and affiliated deposits, (ed.) L. Corriveau, E.G. Potter and A.H. Mumin; Geological Association of Canada, Special Paper 52.

Cuney, M., 2010. Evolution of uranium fractionation processes through time: driving the secular variation of uranium deposits; Economic Geology, v. 105, p. 553–569.

Duffett, C.L., Potter, E.G., Petts, D.C., Acosta-Gongora, P., Cousens, B.L., Sparkes, G.W. 2020. The evolution of metasomatic uranium ore systems in the Kitts-Post Hill belt of the Central Mineral Belt, Labrador, Canada; Ore Geology Reviews, 126, 103720.

Fayek, M., and Kyser, T.K., 1997. Characterization of multiple fluid-flow events and rare-earth-element mobility associated with formation of unconformity-type uranium deposits in the Athabasca Basin, Saskatchewan; The Canadian Mineralogist, v. 35, p. 627–658.

Frimmel, H.E., Schedel, S., and Brätz, H., 2014. Uraninite chemistry as forensic tool for provenance analysis; Applied Geochemistry, v.48, p. 104–121.

Fryer, B.J., and Taylor, R.P., 1987. Rare earth elements distributions in uraninites: implications for ore genesis; Chemical Geology, v. 63, p. 101–108.

Gandhi, S.S., 2003. An overview of the Fe oxide-Cu-Au deposits and related deposit types; Canadian Institute of Mining and Metallurgy Conference, Montreal, Canada.

Gandhi, S.S., Potter, E.G., and Fayek, M., 2018. New constraints on genesis of the polymetallic veins at Port Radium, Great Bear Lake, Northwest Canadian Shield; Ore Geology Reviews, v. 96, p. 28–47.

Griffin, W.L., Powell, W.J., Pearson, N.J., and O'Reilly, S.Y., 2008. GLITTER: Data reduction software for laser ablation ICP-MS; *in* Laser Ablation ICP-MS in the Earth Sciences: Current practices and outstanding issues, (ed.) P. Sylvester; Mineralogical Association of Canada, Short Course Series, 40, p. 307–311.

Guillong, M., Hametner, K., Reusser, E., Wilson, S.A., and Günther, D., 2005. Preliminary characterisation of new glass reference materials (GSA-1G, GSC-1G, GSD-1G and GSE-1G) by laser ablation-inductively coupled plasma-mass spectrometry using 193 nm, 213 nm and 266 nm wavelengths; Geostandards and Geoanalytical Research, v. 29, p. 315–331.

Hidaka, H., and Gauthier-Lafaye, F., 2001. Neutron capture effects on Sm and Gd isotopes in uraninites; Geochimica et Cosmochimica Acta, v. 65, p. 941–949.

Hidaka, H., Hollinger, P., Shimuzu, H., and Masuda, A., 1992. Lanthanide tetrad effect observed in the Oklo and ordinary uraninites and implication for their forming processes; Geochemistry Journal, v. 26, p. 337–346.

Hildebrand, R.S., 1986. Kiruna-type deposits: their origin and relationship to intermediate subvolcanic plutons in the Great Bear magmatic zone, Northwestern Canada; Economic Geology, v. 81, p. 640–659.

Hoffman, P., and Hall, L., 1993. Geology, Slave craton and environs; District of Mackenzie, Northwest Territories; Geological Survey of Canada, Open File 2559, scale 1:1,000,000.

Jackson, S.E., 2008. Calibration strategies for elemental analysis by LA-ICP-MS; *in* Laser ablation-ICP-mass spectrometry in the Earth sciences: current practices and outstanding issues, (ed.) P. Sylvester; Mineralogical Association of Canada, Short Course Series 40, p. 169–188.

Jackson, S.E., and Cabri L.J., 2011. Progress in quantitative determination and mapping of trace elements in sulfides minerals using LAICPMS; Geological Association of Canada-Mineralogical Association of Canada joint annual meeting, Ottawa, Program with Abstracts, v. 34, p. 101–102.

Jochum, K.P., Willbold, M., Raczek, I., Stoll, B., and Herwig, K., 2005. Chemical characterisation of the USGS reference glasses GSA-1G, GSC-1G, GSD-1G, GSE-1G, BCR-2G, BHVO-2G and BIR-1G using EPMA, ID-TIMS, ID-ICP-MS and LA-ICP-MS; Geostandards and Geoanalytical Research, v. 29, p. 285–302.

Lach, P., Mercadier, J., Dubessy, J., Boiron, M-C., and Cuney, M., 2013. In situ quantitative measurement of rare earth elements in uranium oxides by laser ablation-inductively coupled plasma-mass spectrometry; Geostandards and Geoanalytical Research, v. 37, p. 277–296.

Maas, R., and McCulloch, M.T., 1990. A search for fossil nuclear reactors in the Alligator River uranium field, Australia: constraints from Sm, Gd and Nd isotopic studies; Chemical Geology, v. 88, p. 301–315.

Mercadier, J., Cuney, M., Lach, P., Boiron, M.-C., Bonhoure, J., Richard, A., Leisen, M., and Kister, P., 2011. Origin of uranium deposits revealed by their rare earth element signature; Terra Nova, v. 23, p. 264–269.

Montreuil, J.-F., Corriveau, L., and Potter, E.G., 2015. Formation of albitite-hosted uranium within IOCG systems: The Southern Breccia, Great Bear magmatic zone, Northwest Territories, Canada: Mineralium Deposita, v. 50, p. 293–325.

Montreuil, J.-F., Corriveau, L., and Davis, W., 2016a. Tectonomagmatic evolution of the southern Great Bear magmatic zone (Northwest Territories, Canada) – Implications on the genesis of iron oxide alkali-altered hydrothermal system; *in* Proterozoic iron oxide-apatite (± REE) and iron oxide-copper-gold and affiliated deposits of Southeast Missouri, USA, and the Great Bear magmatic zone, Northwest Territories, Canada, (ed.) J. Slack, L. Corriveau and M. Hitzman; Economic Geology, v. 111, p. 2111–2138.

Montreuil, J.-F., Corriveau, L., Potter, E.G., and De Toni, A.F., 2016b. On the relation between alteration facies and metal endowment of iron oxide–alkali–altered systems, southern Great Bear magmatic zone (Canada) ; *in* Proterozoic iron oxide-apatite (± REE) and iron oxide-copper-gold and affiliated deposits of Southeast Missouri, USA, and the Great Bear magmatic zone, Northwest Territories, Canada, (ed.) J. Slack, L. Corriveau and M. Hitzman; Economic Geology, v. 111, p. 2139–2168.

Mumin, A.H., Somarin, A.K., Jones, B., Corriveau, L., Ootes, L., and Camier. J., 2010. The IOCG-porphyry-epithermal continuum of deposits types in the Great Bear magmatic zone, Northwest Territories, Canada; *in* Exploring for iron oxide copper-gold deposits: Canada and global analogues, (ed.) L. Corriveau and A.H. Mumin; Geological Association of Canada, Short Course Notes, No. 20, p. 59–78.

Ootes, L., Goff, S., Jackson, V.A., Gleeson, S.A., Creaser, R.A., Samson, I.M., Evensen, N., Corriveau, L., and Mumin, A.H., 2010. Timing and thermochemical constraint on multi-element mineralization at the Nori/RA Cu-Mo-U prospect, Great Bear magmatic zone, Northwest Territories, Canada; Mineralium Deposita, v. 45, p. 549–566.

Pagel, M., Pinte, G., and Rotach-Toulhoat, N., 1987. The rare earth elements in natural uranium oxides; Monograph Series on Mineral Deposits, v. 27, p. 81–85.

Potter, E.G., Montreuil, J.-F., Corriveau, L., and De Toni, A., 2013. Geology and hydrothermal alteration of the Fab Lake region, Northwest Territories; Geological Survey of Canada, Open File 7339, 26 p.

Potter, E.G., Montreuil, J.-F., Corriveau, L., and Davis, W.J., 2019. The Southern Breccia metasomatic uranium system of the Great Bear magmatic zone, Canada: iron oxide-copper-gold (IOCG) and albitite-hosted uranium linkages; *in* Ore deposits: origin, exploration, and exploitation, (ed.) S. Decrée and L. Robb; Geophysical Monograph 242, First Edition, John Wiley and Sons Inc., p. 109–132.

Potter, E.G., Acosta-Góngora, P., Corriveau, L., Montreuil, J.-F. and Yang, Z., in press. Uranium enrichment processes in metasomatic iron oxide and alkali-calcic systems as revealed by uraninite trace element chemistry; *in* Mineral systems with iron oxide copper-gold (IOCG) and affiliated deposits, (ed.) L. Corriveau, E.G. Potter and A.H. Mumin; Geological Association of Canada, Special Paper 52.

Pouchou, J.L., and Pichoir, F., 1984. Un nouveau modèle de calcul pour la microanalyse quantitative par spectrométrie de rayons X – Partie II : application à l'analyse d'échantillons hétérogènes en profondeur; La Recherche Aérospatiale, v. 5, p. 349–367.

Richards, J.P., and Mumin, A.H., 2013. Lithospheric fertilization and mineralization by arc magmas: Genetic links and secular differences between porphyry copper ± molybdenum ± gold and magmatic-hydrothermal iron oxide copper-gold deposits; *in* Tectonics, metallogeny, and discovery: the North American cordillera and similar accretionary settings, (ed.) M. Colpron, T. Bissig, B.G. Rusk and J.F.H. Thompson; Society of Economic Geologists, Special Publication 17, p. 277–299.

Somarin, A.K., and Mumin, A.H., 2012. The Paleoproterozoic high heat production Richardson granite, Great Bear magmatic zone, Northwest Territories, Canada: source of U for Port Radium?; Resources Geology, v. 62, p. 227–242.

Spano, T.L., Simonetti, A., Wheeler, T., Carpenter, G., Freet, D., Balboni, E., Dorais, C., Burns, P.C., 2017. A novel nuclear forensic tool involving deposit type normalized rare earth element signatures; Terra Nova, 29, 294-305.

Williams, P.J., 2010. Classifying IOCG deposits; *in* Exploring for iron oxide copper-gold deposits: Canada and global analogues, (ed.) L. Corriveau A.H. Mumin; Geological Association of Canada, Short Course Notes, No. 20, p. 13–22.

Data Tables (see digital versions)

Appendix A. Electron probe microanalyses (EMPA) of uraninite.

Appendix B. Laser ablation-inductively coupled plasma-mass spectrometry (LA-ICP-MS) of uraninite